Induced currents and AC losses models for a butt-joint with Rutherfords shunts

A. Torre, T. Schild, E. Gaxiola, P. Decool, G. Jiolat

***Abstract*— The ITER Central Solenoid (CS) has terminal butt-type joints called Coaxial joints. It was decided to study a design of this joint with rutherford shunts, and to build models for its resistive and inductive behaviors. In particular, the behavior of the joint under magnetic field transients is investigated with various analytical models that are compared with a FEM model. The key point of the study was to verify that the induced currents were reasonable and would not induce flux jumps in the rutherfords. A prototype with simplified geometry was tested in the CEA Josefa facility under various field ramps. The results are presented and discussed.**

***Index Terms*— Nuclear Fusion, Superconducting Joints.**

I. Introduction

THE ITER Central Solenoid (CS) is composed of six modules, each one a stack of 6 hexa-pancakes and one quad-pancake. A module has thus 6 internal joints, of butt-type configuration, which are called splice-joints. The two terminals of each module are connected to vertical superconducting extension lengths that are in turn connected to the feeder system. The connection to the extension length is made using another butt-joint configuration called "Coaxial Joint". Two designs are considered for this joint: The baseline Laced-Union Design (LUD) and the Parallel Rutherfords Design (PRD). The work presented here tries to summarize the approaches to model the AC losses and induced currents loops in the two design, with the aim of evaluating whether the recent design is still acceptable with regards to transient magnetic field during operation.

II. Coaxial Joints Designs Description

A. Joint Specification and General Description

The CS coaxial joint must electrically connect two compacted Nb_3Sn CS cables facing each other in a butt-type geometry, while achieving a DC resistance below 4.1 nΩ. To achieve this, the cables are initially compacted in a copper tube (crimp tube) to form a terminal lead. Then, a superconducting shunt is added to bypass both leads positioned head-to-head. In the two designs studied here, one uses a cylindrical layer of twisted strands (LUD), while the other uses straight rutherfords (PRD). In both designs, the superconductors are embedded in copper shells, compacted or soldered to the lead.

B. Original LUD Design

The LUD baseline design for this joint has been studied, tested and analyzed in detail in the past years (see [1]-[4]). Its design will not be detailed here, but its main components are illustrated in Fig. 1. It should be noted that, in this design, the laced union is soldered to the terminal lead.

Fig. 1. LUD joint design (courtesy David Everitt)

For the analyses lead hereafter, the useful characteristics of this design are summarized below:

TABLE I
Coax-LUD Parameters

Name	Value	Unit
Joint total length	355	[mm]
Laced Union strands twist pitch	1200	[mm]
Laced Union inner radius	16.55	[mm]
Outer copper shell average thickness	5	[mm]

C. PRD Design

A new design has been proposed to try to simplify part of the assembly process by the use of straight superconducting shunts (rutherfords) and the use of indium wire compaction instead of soldering. Again, the details of the design will not be presented, but Fig. 2 and Table II give the important information for our calculations. It should also be noted that the design illustrated is not the final one and is only indicative of the concept used. In particular, the number of rutherfords (2 or 4) is still uncertain, and in the model proposed in section IV. C., we will consider only 2 rutherfords shunts in parallel (one top and one bottom in Fig. 2.).

A. Torre, P. Decool and G. Jiolat are with CEA, IRFM, F-13108 Saint-Paul-Lez-Durance, France (+33442257442 email: alexandre.torre@cea.fr).
T. Schild and E. Gaxiola are with the ITER Organisation, St-Paul-Lez-Durance, France.
The views and opinions expressed herein do not necessarily reflect those of the ITER Organization

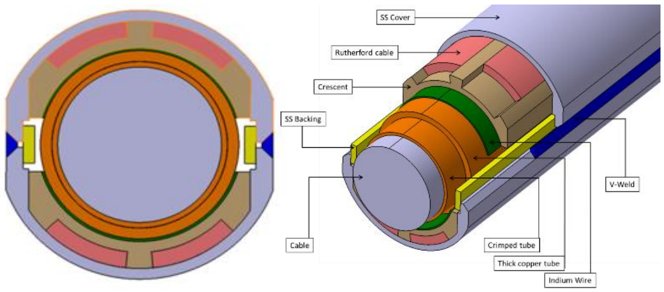

Fig. 2. Cross section and sub-elements of PRD joint

TABLE II
COAX-PRD PARAMETERS

Name	Value	Unit
Joint total length	355	[mm]
Rutherfords width	18	[mm]
Rutherfords inner radius	20	[mm]
Rutherfords twist pitch	120	[mm]

III. DC Resistance Considerations

A. Materials DC resistance

Although DC resistance is not the main goal of the models described in this paper, it is important to evaluate the resistive paths in order to include their influence in the inductive behavior. The resistance of a cylindrical shell defined by its inner radius r_1, outer radius r_2, length L and resistivity ρ is simply $R_{mat} = \rho/(2\pi L)ln(r_1/r_2)$. Taking $\rho_{Cu} = 2.5\ 10^{-10}\ \Omega.m$ and $\rho_t = 1\ 10^{-9}\ \Omega.m$ for the copper and cable transverse resistivities respectively we find 0.28 nΩ and 0.30 nΩ for the LUD and PRD joints. The resistivities are only indicative (not measured), but give an estimate of the materials contribution to DC resistance.

B. Interfaces resistance

While estimating the interfaces (contact, solder etc…) resistance from the geometry is not relevant, we know from the experimental values (on the LUD joint, see [3]) that they are dominating the DC resistance. Therefore, we propose to add to the material resistance R_{mat} an interface resistance R_{int} in the form a resistive barrier homogeneous on the cylindrical surface of the joint. If we take the interface at a radial position of 18.7 mm (position of the crimp tube), the cylindrical surface of the joints amounts to $S_j = 16283\ mm^2$, and we get:

$$\rho_b e_b = R_{int} * S_j$$

Where $\rho_b e_b$ defines the interface resistance in $\Omega.m^2$. In this case, for R_{int} =1 nΩ, we have $\rho_b e_b = 8.14\ 10^{-12}\ \Omega.m^2$.

IV. AC Losses and Induced Currents

A. Introduction

It is important to note that while the PRD Design was proposed to simplify the joint assembly process and get a more reliable DC resistance, its inductive behavior was never assessed experimentally. In particular, this joint will be subject to magnetic field variations of about 0.1 T/s during one second in both transverse and parallel directions. Furthermore, analytical models to represent the inductive behavior of these joints are necessary to calculate the heat loads during operation, which is generally done by implementing AC losses models in a thermohydraulic code. Finally, one key point was to verify that the PRD design is not subject to high circulating currents which could lead to flux jumps during operation.

B. LUD Joint AC losses model in transverse field transient

Since the LUD joint is surrounded by a twisted superconducting layer, we propose for this joint an AC model relying on the composite (strand) model described partly in [5] and illustrated in the equations and figure below.

$$\theta_{Cu} = \frac{\mu_0}{8.\rho_{Cu}} \frac{{R_2}^4 - {R_1}^4}{{R_2}^2}$$

$$\theta_{Sc} = \frac{\mu_0}{2\rho_t}\left(\frac{L_p}{2\pi}\right)^2\left(\frac{R_1}{R_2}\right)^2$$

$$\theta_{Sc/Cu} = \frac{\mu_0}{2\rho_{Cu}}\left(\frac{L_p}{2\pi}\right)^2\left(\frac{R_1}{R_2}\right)^2\frac{{R_2}^2 - {R_1}^2}{{R_2}^2 + {R_1}^2}$$

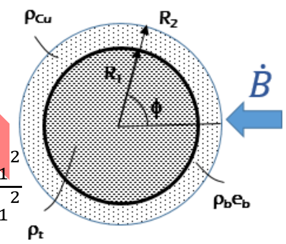

Fig. 3. Composite model (with twist pitch L_p) and time constants definition

Where θ_{Cu} is linked with eddy currents, θ_{Sc} is linked with coupling currents and $\theta_{Sc/Cu}$ is linked with the induced currents in the outer copper shell. This model describe both the internal field B_i and the power P dissipated by the following equations:

$$B_i = B_a - \theta_r \dot{B_i}\ \ ;\ \ P = \frac{2\theta_r \dot{B_i}^2}{\mu_0}$$

Where B_a is the external applied field, and θ_r is the sum of all time constants contributing to the losses. In the case of the LUD joint, considering that the laced union shields the rest of the cable, we get $\theta_r = 18$ s. Furthermore, the shielding currents in this model have a cosine distribution and can be expressed as a linear current density:

$$J_L = \dot{B_i}\left(\frac{L_p}{2\pi}\right)^2\frac{1}{\rho_t}\cos(\phi) = \frac{2\theta_r \dot{B_i}}{\mu_0}\cos(\phi)\ [A/m]$$

The calculation of the internal field through the differential equation above permits the evaluation of the losses and induced currents. For a 0.1 T/s ramp during one second, followed by a plateau at constant field, we get:

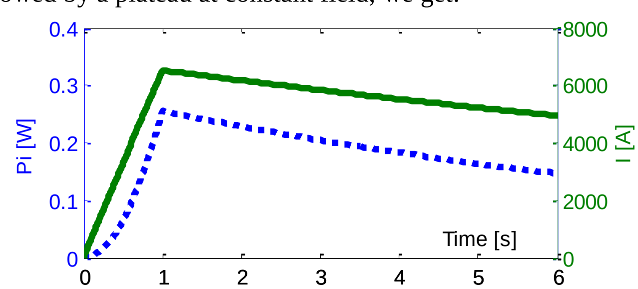

Fig. 4. Calculated power and induced current in the LUD joint

The figure above shows that losses calculated with B_i (around 0.25 W) are much lower than the approximation with B_a (around 90 W). The figure gives also the total screening current for one half of the laced union. Of course, the most critical part of the laced union is the one perpendicular to the changing field, in which the current will rise to around

200 A/mm, which seems sustainable by the two layers of 0.8 mm diameter strands that compose the laced union.

C. PRD joint AC losses model under transverse field

It is trickier to estimate the losses for this design since we cannot rely on models related to composites (circular geometry, uniform internal field) as for LUD. Since the rutherfords are parallel and define an equipotential on each side of the joint, we propose to represent the screening of the external field by a 1D diffusion equation of the field in the longitudinal direction of the joint, with in this case, linear time-dependent Dirichlet boundary conditions:

$$\Delta B - \frac{\mu_0}{\rho}\frac{\partial B}{\partial t} = 0$$
$$with\ B(0,t) = B(L_j,t) = \dot{B}_a t$$

Where $\dot{B}_e$ is the constant time derivative of the external field (for our current case study, $\dot{B}_a$= 0.1 T/s). The solution, given in terms of eigenfunction expansion, takes the form:

$$B(x,t) = \dot{B}_a.t + \frac{2\dot{B}_a.L_j{}^2}{\pi^3\alpha^2}\sum_{\substack{n=1\\ n\ odd}}^{\infty}\frac{1}{n^3}\left(e^{-\alpha^2\left(\frac{n\pi}{L_j}\right)^2 t} - 1\right) sin\left(\frac{n\pi x}{L_j}\right)$$

Where $\alpha = (\rho/\mu_0)^{1/2}$. When $B(x,t)$ is known, the transverse current density between the two rutherfords $J_t(x,t)$ is simply deduced by a Maxwell-Ampere law, and the circulating current in the rutherfords is found by integration along x:

$$I(x,t) = \frac{2wB_a.L_j{}^2}{\mu_0\pi^3\alpha^2}\sum_{n=1}^{\infty}\frac{1}{n^3}\left(e^{-\alpha^2\left(\frac{n\pi}{L_j}\right)^2 t} - 1\right) sin\left(\frac{n\pi x}{L_j}\right)$$

Where w is the width of the screened volume (here we will take the width of the rutherfords). Since the equation is 1D, a demagnetization factor (taken equal to 2 between slab and rod geometry, see [9]) is needed to represent the 3D geometry. The equations above give the field and current distributions of Fig. 5 for the usual case of 0.1 T/s during 1 s followed by a plateau.

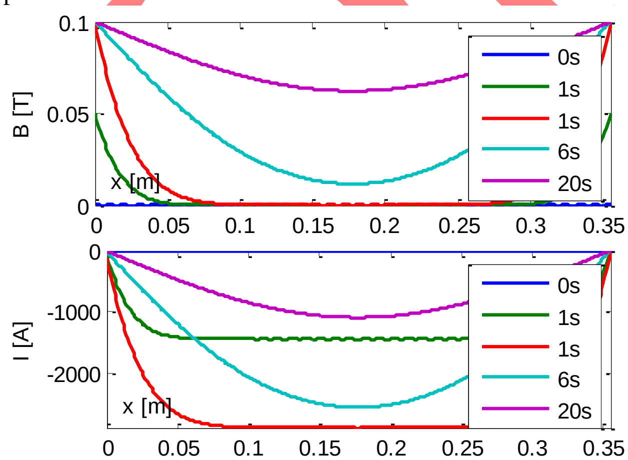

Fig. 5. Field and induced current spatial distribution in PRD joint.

If we take a transverse resistivity inside the cable of ρ_t = 1 10^{-9} Ω.m, we can calculate the power dissipated in the joint during the field ramp.

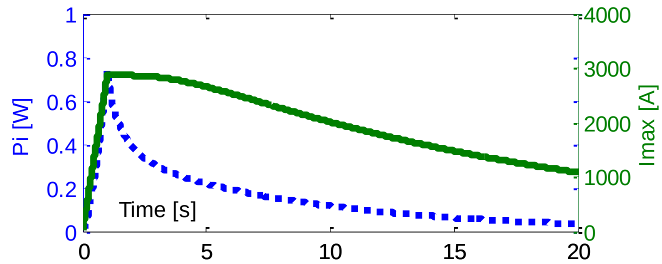

Fig. 6. Calculated power and induced current in the PRD joint

These values are in good agreement with a COMSOL FEM model of the joint, illustrated in Fig. 7, subject to the same field change.

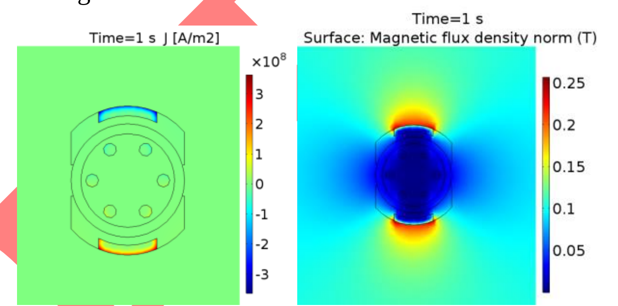

Fig. 7. COMSOL calculation of induced current (left) and field map (right) in the PRD joint.

D. PRD joint AC losses under axial field

The joint will also be subject to changing axial field of about 0.1 T/s. There are no pure analytical models for the axial losses, and to give an idea, one can calculate the magnetic energy for ΔB = 0.1 T field variation by $E_{mag}=\Delta B^2/\mu_0$ which gives about 1.9 J deposited in the full joint for a perfect shielding. Considering an adiabatic deposit, without considering the helium, this corresponds to a temperature increase to about 7 K. When considering helium, it becomes negligible. Now for the induced currents in this configuration, we had to rely on our COMSOL model (illustrated in Fig. 7). The integration of current density in the rutherford region gives less than 100 A carried by the rutherford as the shielding currents in the cable loop through these superconducting shunts.

V. Experimental Campaign & Model Validation

A. Sample design and manufacture

Since no PRD joint had been manufactured or tested, we decided to build a simplified mockup, with only two straight rutherfords soldered after heat treatment on a copper bar representative of the joint geometry (see Fig. 8).

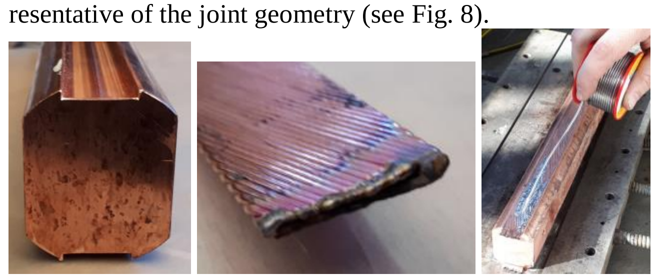

Fig. 8. PRD Mockup manufacturing process

Then, the mockup was instrumented with a pickup coil and tested in the JOSEFA facility, where a superconducting dipole can apply an external varying field up to around 1 T/s. The pickup has 21 turns (n_s) and a cross sectional area of 1.63 10^{-2} m^2 (S_s).

B. Test Campaign

There were two main interests in this test campaign. First, we would be able to cross-check our 1D analytical model and see if it is consistent with the more complex geometry of the joint. Then, we would also be able to increase the field-variation rate, and see if some instabilities (flux-jumps) arise. The test program included background fields B_e of 0.1 T, 0.4 T, 0.6 T and 0.8 T with ramp-up times of 1 s, 2 s, 5 s and 10 s for each. The sample pickup coil voltage Vs gives us access to an effective magnetization defined by:

$$M_{eff} = B_e - \int_0^t \frac{V_s}{n_s S_s} dt$$

The field ramps and measured magnetizations are shown in the Fig. 9.

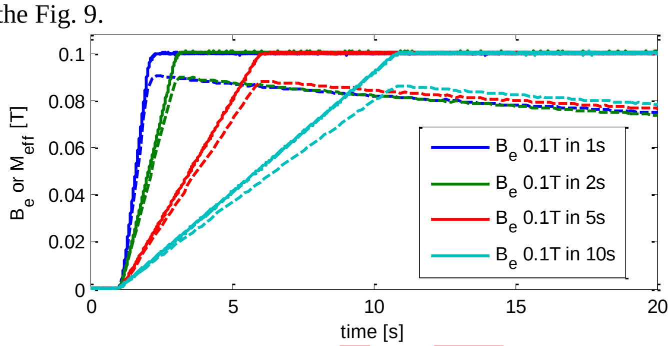

Fig. 9. B_e = 0.1 T runs: B_e plain lines / M_{eff} dashed lines

The curves for other background fields are similar, and, just looking at M_{eff}, no thermal instabilities are visible. Nevertheless, when looking at the sample pickup voltage directly, the sensitivity is higher (before integration), and for 0.6 T runs, we start to see fluctuations of the signal which could indicate the onset of flux jumping phenomena (see Fig. 10).

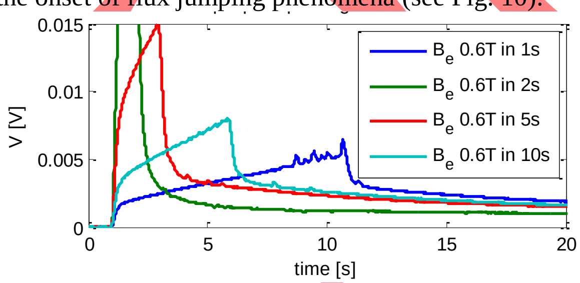

Fig. 10. Pickup voltages for B_e= 0.6 T runs

C. Model-Experiment comparison

Using the 1-D diffusion model above to calculate the flux, we can model the induced voltage in the experiment and compare with experimental values. The field inside the sample was considered homogeneous in the cross-section, and decreasing linearly in the rutherfords thickness. With these assumptions, the model gives good agreement with the measured voltages as shown in Fig. 11 for 0.1 T runs.

This comparison validates the model, and gives confidence in the predicted induced currents I_{ruth} and losses values. Knowing the resistivity of the copper used for the sample, we can also deduce the power dissipated P_{tot}. We also made a fully adiabatic evaluation of the maximum copper temperature rise T_{max}, although without the helium enthalpy, this temperature is very pessimistic.

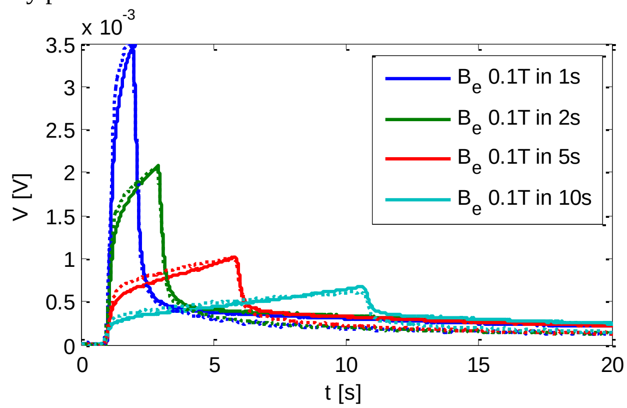

Fig. 11. Modeled (dashed) and experimental (plain) pickup voltages for B_e= 0.1T runs

TABLE III
MODEL LOSSES CALCULATION FOR T=1S RUNS

Runs	I_{ruth} [kA]	$P_{tot\ max}$ [W]	$E_{tot\ 1s}$ [J]	$E_{tot\ 20s}$ [J]	$T_{max\ 1s}$ [K]	$T_{max\ 20s}$ [K]
B_e = 0.1 T	3.19	0.084	0.037	0.50	5.65	8.13
B_e = 0.4 T	12.8	1.35	0.61	8.00	12.4	18.1
B_e = 0.6 T	19.9	3.26	1.52	19.4	15.9	22.3
B_e = 0.8 T	25.6	5.40	2.51	32.1	18.1	25.0

These values show that with ramp rates of around 0.1 T/s during 1 s, the induced currents are acceptable for this joint configuration, even including a maximum of 100 A induced by axial field variations. Therefore, there should be no instabilities arising in this design. The adiabatic temperature values are obviously pessimistic, but show that for higher ramp-rates, a badly cooled joint could be subject to high heat loads that might lead to flux jumping.

VI. CONCLUSION

The CS Coaxial joint is a critical sub-element of the crucial ITER Central Solenoid system. In the frame of the assembly preparation, an alternative design (PRD) is investigated, which makes use of parallel rutherford shunts. Since this design is not tested up to now, models had to be developed to check that circulating currents and AC losses were comparable to the previous design, and acceptable for the joint operation. A 1D diffusion model is proposed and validated on experimental data in the Josefa facility. Using this model, the currents and losses are calculated and show that the design is sound and should not suffer from thermal instabilities in the ramp-rates considered in operation.

References

[1] N. Martovetsky et. al, “R&D Effort for ITER Central Solenoid”, IEEE 26th Sympposium on Fusion Engineering, 2015.

[2] I. Aviles Santillana et. al, “ Examination of ITER Central Solenoid prototype joints” , Fus. Eng and Des. *Article in Press*.

[3] N. Martovetsky et. al, “ Performance of ITER CS Joints ” , *MT25 Conference Presentation.*

[4] N. Martovetsky et. al, “ Development of the Joints for ITER Central Solenoid ”, *IEEE Trans. Applied Supercond.*., vol. 21, no. 3, Jun. 2011.

[5] J.L. Duchateau et. al, “Coupling-current losses in composites and cables: analytical calculations”, Handbook of Applied Superconductivity, Volume 2, IoP, 1998.

[6] L. Zani et. al, “Status of CEA Magnet Design Tools and Applications to EU DEMO PF and CS Magnets”, IEEE Trans on Applied Supercond. vol. 28, No. 3, April 2018.

[7] D. Ciazynski et. al, “ Electrical and Thermal Designs and Analyses of Joints for the ITER PF Coils ”, IEEE

[8] P. Decool et. al, “The CEA JOSEFA Test Facility for Subsize Conductors and Joints”, IEEE Trans on Applied Supercon., vol. 14, no. 2, June 2004.

[9] J.P. Soubeyrand, B. Turck, “Losses in superconducting composites under high rate pulsed transverse field”, IEEE Trans. on Mag., vol. MAG-15, No. 1, January 1979.